primitive bombardier beetle, the ozaenine *Goniotropis nicaraguensis*, which discharges its hot quinones as an unpulsed stream (*14*).

We postulate that the individual pulsations represent individual microexplosions, repeated one after the other as the beetle delivers its spray. Critical to the operation of such a cyclic mechanism is the maintenance of continuous pressure on the reservoir through sustained contraction of its musculature and an oscillatory opening and closing of the valve that controls access to the reaction chamber. We envision this valve oscillation to proceed passively. At the outset of events leading to an ejection, pressure from the reservoir overcomes the passive occlusory force of the valve, causing fluid to flow into the reaction chamber. This leads to a quick buildup of pressure in the chamber (as a consequence of both the oxygen liberated from hydrogen peroxide and the temperature increase) (*5*) with the result that the valve is forced closed. As pressure continues to build up in the chamber, a point is reached at which the chamber vents itself, shooting out its contents. With the chamber again below the feeding pressure of the reservoir, the cycle is reinitiated [and proceeds as diagrammed in Fig. 2: (A) → (B) → (C)]. Preliminary structural work shows the valve to be a one-way conduit, with an exit port projecting into the reaction chamber and guarded by what are essentially compressible lips (*15*). The oscillatory mechanism is thus virtually automatic. To effect an ejection, the beetle needs to control only the duration of compression of the reservoir, which it could achieve by conventional neuromuscular action.

From an adaptive point of view, a pulsed delivery system offers several advantages over a continuous discharge mechanism. First, it provides for a high discharge velocity without requiring muscles to supply the necessary pressure. Precursors can be supplied at low pressure; the chemical reaction generates the high pressure for propelling the discharge. The second advantage, related to the first, concerns the separation of control and propulsion functions. Muscle force shows low-pass characteristics; providing high forces generally involves a reduction in the precision of temporal control (*16*). Because the bombardier beetle does not use muscles to provide propulsion, the control function can be more accurate: short discharges can be produced without reduction in spray velocity. Spray delivery can thus be maintained constant over time, with the length of the pulse train adjusted to the magnitude and duration of an attack. Finally, the discontinuity of the reaction, inasmuch as it would provide for repetitive cooling of the reaction chamber through periodic introduction of reactants, could protect the enzymes from thermal denaturation.

A striking technological analog of the bombardier beetle is provided by the notorious V-1 "buzz" bomb of World War II (*17*). Both the beetle and the V-1 engender a pulsed jet through an intermittent chemical reaction, and both have passively oscillating valves controlling access to their reaction chambers. For a propelled vehicle such a system is suboptimal because thrust is discontinuous. For the bombardier beetle the appropriate measure is not thrust but rather production of an effective deterrent with good control and high discharge velocity, with investment of minimal muscular force. For this purpose the pulsed mechanism is ideal.

REFERENCES AND NOTES

1. T. Eisner, *J. Insect. Physiol.* **2**, 215 (1958).
2. J. Dean, *J. Comp. Physiol.* **135**, 51 (1980).
3. H. Schildknecht, *Angew. Chem.* **69**, 62 (1957).
4. ——— and K. Holoubek, *ibid.* **73**, 1 (1961); H. Schildknecht, E. Maschwitz, U. Maschwitz, *Z. Naturforsch. Teil B* **23**, 1213 (1968).
5. D. J. Aneshansley, T. Eisner, J. M. Widom, B. Widom, *Science* **165**, 61 (1969).
6. J. O. Westwood, *An Introduction to the Classification of Insects* (Longmans, London, 1839).
7. We caused tethered beetles to discharge by pinching individual legs with forceps (Fig. 1A). The recording system consisted of a microphone (±12 dB from 1 to 100 kHz with a sensitivity of 26 μV/μbar at 4 kHz), positioned at 2.5 cm above the abdominal tip of the beetle; an amplifier (model 255 low noise amplifier, Ithaco); and a recorder (Lockheed magnetic tape recorder, model 417D; tape speed = 30 inches per second).
8. For analyses (Kay Elemetrics sonograph, model 7029A) recordings were replayed (wide band setting) at 1/8 recording speed (frequency range, 0.16 to 16 kHz, or 1.28 to 128 kHz at recorded speed).
9. E. Meyer and E.-G. Neumann, *Physical and Applied Acoustics: An Introduction* (Academic Press, New York, 1972).
10. Piezoelectric bimorph (Vernitron Piezoelectric Division, PZT-5B), mounted as a cantilever beam (1.25 cm long, 0.3 cm wide).
11. We again induced tethered beetles to discharge by pinching individual legs with forceps (Fig. 1A). The acoustical detection system was as described (7). The piezoelectric crystal was buffered (Picometric amplifier model 181, Instrumentation Laboratory, Inc.) and amplified (model 255 low noise amplifier, Ithaco). Both microphone and crystal outputs were recorded at 15 inches per second (Lockheed magnetic tape recorder, model 417D). The crystal was positioned 0.5 to 0.75 cm from the abdominal tip of the beetle, along the anticipated trajectory of the spray (the line from the abdominal tip to the site on the beetle's leg pinched with forceps).
12. The speed (in frames per second) was set by the repetition rate of stroboscopic flashes used for illumination.
13. The velocity was calculated from tracings of the advancing spray front, as depicted in enlarged projections of the first two film frames of individual pulses.
14. T. Eisner and D. J. Aneshansley, *Science* **215**, 83 (1982).
15. T. Eisner, unpublished scanning electron microscopic observations.
16. R. B. Stein, *Nerve and Muscle* (Plenum, New York, 1980).
17. A. Barker, T. R. F. Nonweiler, R. Smelt, *Jets and Rockets* (Chapman and Hall, London, 1959).

18. Supported by NIH grant AI 02908 and a Ford Foundation postdoctoral fellowship (to J.D.). We thank C. Miller for help with the cinematography, M. Eisner for assistance, and R. Hoffmann and F. Bogner for critical readings of the manuscript. We dedicate this paper affectionately to the memory of the late Kenneth Roeder, with whose help we made our first acoustical recordings of bombardier beetle discharges.

23 January 1990; accepted 27 March 1990

Electrophoresis of Flexible Macromolecules: Evidence for a New Mode of Transport in Gels

DAVID L. SMISEK AND DAVID A. HOAGLAND

Movement of macromolecules through low concentration agarose gels was investigated with linear poly(styrenesulfonate), linear DNA, star-shaped poly(styrenesulfonate), and circular DNA. Mobilities of weakly entangled flexible macromolecules were independent of molecular radius; within a homologous chemical sequence, electrophoretic separation at low field strengths depended solely on the degree of polymerization. These observations cannot be explained either by sieving or by reptation mechanisms; transport was apparently controlled by spatial variations of chain configurational entropy. Only when the chain was highly entangled did chain topology affect mobility. Evidence for entropically regulated transport clarifies how gel electrophoresis separates flexible macromolecules.

ALTHOUGH GEL ELECTROPHORESIS IS invaluable for fractionating biopolymers, the molecular mechanisms by which separation occurs are still not well understood. Chain entanglement plays a prominent role; thus, we defined three entanglement regimes for a relaxed, flexible macromolecule surrounded by a random gel (Fig. 1). A chain is unentangled when its mean

Department of Polymer Science and Engineering and Department of Chemical Engineering, University of Massachusetts, Amherst, MA 01003.

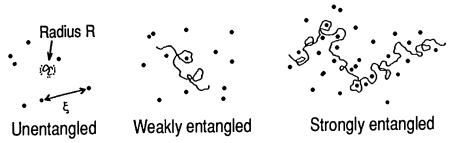

Fig. 1. Representation of the three entanglement regimes. The solid dots represent the gel network, while the solid line represents the polymer chain.

molecular radius (R) is much smaller than the average mesh spacing (ζ) of the gel. When these two lengths are comparable, the chain can be viewed as weakly entangled, and when R is much greater than ζ, the chain is strongly entangled.

For strong entanglement (Fig. 1), the reptation model can be used, in which the complex gel media is replaced by a fictitious "tube" that envelops the chain (*1, 2*). Translational motion of the molecule is thereby restricted to one dimension, along the curvilinear contour of the tube. For the unentangled and weakly entangled regimes (Fig. 1), separation during electrophoresis has been explained by a sieving model (*3, 4*), in which a migrating polymer chain can be viewed as a hard sphere undergoing biased Brownian motion. An electrophoresis gel can reasonably be modeled as a matrix of randomly oriented and positioned fibers; the sphere mobility is assumed to be proportional to the fractional volume of this matrix that is accessible to the sphere. These simplifications imply that the electrophoretic mobility (μ) in a random fiber array is an exponential function of the product of the fiber concentration (ϕ) and the square of the sphere (ρ) plus fiber (r) radii (μ_0 = mobility in the absence of gel; A = coefficient)

$$\mu/\mu_0 = \exp[-A\phi(\rho + r)^2]$$

While reasonable for globular proteins, which can behave as inflexible spheres, sieving may be inappropriate to describe separation of flexible or irregularly shaped macromolecules. It has been suggested that for these more complex species, a suitably defined mean molecular radius could provide a basis for interpreting mobility data (*2, 3*) as has been done for gel permeation chromatography.

Therefore, if the sieving model is correct, polymers of identical degree of polymerization (N) (number of repeat units), but different mean molecular radii (R), will exhibit different mobilities. Studies with macromolecules of varying chain topology can be used to test this prediction. We now describe topological effects observed with poly(styrenesulfonate) (PSS) and DNA. Linear PSS exhibits a range of electrophoretic behaviors similar to those of linear DNA (*5, 6*). PSS, however, can be synthesized in an array of topologies not found in natural polymers (*7*).

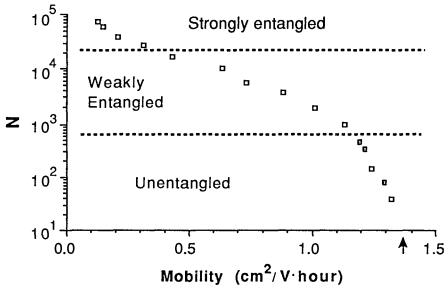

Fig. 2. Dependence of PSS mobility on degree of polymerization N for the three entanglement regimes. Linear PSS molecules were subjected to electrophoresis for 40 hours at 0.3 V/cm through 0.6% agarose in 0.01 M phosphate buffer. The arrow on the abscissa indicates the extrapolation of the mobility to zero N, zero gel concentration, and the free solution mobility as measured by electrophoretic light scattering. The latter two values are independent of N.

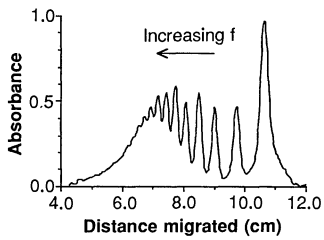

Fig. 3. Densitometry scan at 580 nm of PSS star sample II (N_{arm} = 1000). The sample was subjected to electrophoresis for 6 hours at 0.3 V/cm through 0.6% agarose in 0.01 M phosphate buffer.

Electrophoresis in agarose gels was conducted in the horizontal submarine mode at field strengths below 1.3 V/cm; operating conditions were selected so that the electrophoretic mobility was independent of the magnitude of the applied field. Except for staining, procedures for PSS and DNA were identical. For staining of PSS, the gel was treated with a low concentration of acidic methylene blue solution.

For homologous macromolecules like linear PSS, a plot of N as a function of mobility provides a means of identifying the three entanglement regimes (Fig. 2). We observed the strongly entangled regime ($R >> \zeta$) at the highest molecular size, in the region where the curve of Fig. 2 is concave upward. In the molecular size range for which $R << \zeta$ (Fig. 2, unentangled), mobility differences based on N diminish. Mobility throughout this regime is controlled by the collision frequency of a polymer chain with the gel matrix. During each collision, only one locus of contact exists between polymer and gel; thus, the chain is unentangled. If a macromolecule can be modeled as a hard sphere, this collision process is accounted for in the sieving analysis (*3*), which predicts that mobility approaches its N-independent value in free solution as either N or the gel concentration decreases. These trends were experimentally confirmed for PSS.

The best molecular weight discrimination is observed in the weakly entangled regime ($R \approx \zeta$) (Fig. 2). Mobility data for the weakly entangled, as well as unentangled, regimes can be correlated by the sieving model (*3*), if we use the excluded volume exponent (ν) as a free parameter. This exponent provides a scaling relation between R and N

$$R \sim N^{\nu}$$

Data for weakly entangled and unentangled regimes (Fig. 2) are best correlated with $\nu = 0.2$. This value is quite unreasonable, since it falls below the value $\nu = 1/3$ for a uniformly dense sphere. In fact, the excluded volume exponent for this system is about 0.55 (*8*). Based on these inconsistencies, we questioned whether R is actually a controlling parameter in the observed electrophoretic separations.

To address this question, we observed the motion of chains which varied only in topology, thus uncoupling R and N. A well-defined set of star-shaped PSS macromolecules has not been examined previously by gel electrophoresis. Star polymers consist of linear arms that are connected at a central attachment site. For a given star, the arms possess a nearly uniform degree of polymerization N_{arm}. The number of arms on a star defines its functionality f; therefore, the total degree of polymerization, N, is equal to $N_{arm} \times f$. Synthesis of star PSS leads to a broad distribution of f (*7*). We examined the spatial distribution of star sample II in a 0.6% agarose gel after electrophoresis (Fig. 3). The rightmost peaks correspond to linear chains (f = 1, 2), while the remainder of the peaks correspond to discrete star fractions of lower mobility, each of a successively larger functionality. The resolution of this separation is perhaps the highest ever achieved in a synthetic, high polymer system.

We next compared the dependence of mobility on N for linear and star PSS (Fig. 4). Surprisingly, over the molecular size range displayed, the mobility depended only on N, and was independent of molecular topology.

The relative sizes of linear and star polymers of equal N can be estimated using the following formula (*9*)

$$\langle R_g^2\rangle_{(star)}^{1/2}/\langle R_g^2\rangle_{(linear)}^{1/2} = \sqrt{3f - 2}/f$$

where $\langle R_g^2\rangle_{(star)}^{1/2}$ and $\langle R_g^2\rangle_{(linear)}^{1/2}$ are the root-mean-square radii of gyration of the two

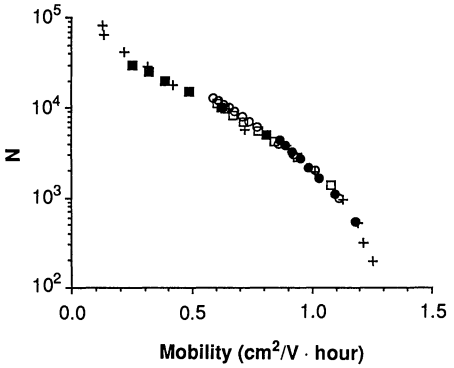

Fig. 4. Mobility of linear and star PSS samples displaying various N values. Star sample I (N_{arm} = 540) (●), star sample II (N_{arm} = 1000) (○), star sample III (N_{arm} = 1400) (□), and star sample IV (N_{arm} = 5000) (■) were subjected to electrophoresis for 7 hours at 1.3 V/cm in 0.6% agarose in 0.01 M phosphate buffer. Linear samples (+) were subjected to electrophoresis for 40 hours at 0.3 V/cm under the same gel conditions.

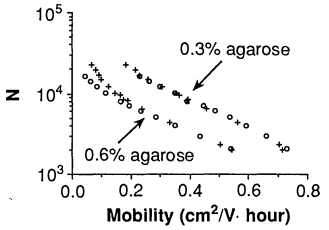

Fig. 5. Mobility of linear (+) and relaxed, circular (○) DNA through 0.3 or 0.6% agarose gels. DNA molecules were subjected to electrophoresis for 30 or 40 hours, respectively, at 0.3 V/cm in 100 mM tris, 90 mM boric acid, and 1 mM EDTA.

topologies. Although rigorously correct only for long chains without electrostatic interactions and excluded volume, this formula will not be greatly in error for polyelectrolytes of low functionality in the high ionic strength solvents used in this study. Superposition of mobility data for the star and linear polymers occurs for all $f \leq 12$, corresponding, at constant molecular size, to a smallest star-to-linear polymer size ratio of about 0.5. According to the sieving theory (*3*), this size ratio will yield a mobility ratio of order 10, a value inconsistent with our data (Fig. 4). We conclude that size measures such as $\langle R_g^2 \rangle^{1/2}$ are superfluous to models for the electrophoretic motion of flexible polymers in the weakly entangled regime.

If these interpretations are correct, linear and relaxed, circular DNA in low concentration agarose gels will behave like PSS topological variants. Ignoring excluded volume and electrostatic effects, $\langle R_g^2 \rangle_{(circle)}$ is equal to one-half $\langle R_g^2 \rangle_{(linear)}$ (*9*). Large mobility differences between the two topologies are, therefore, predicted by the sieving model, even at constant N (for DNA, N is the number of base pairs). We therefore determined whether linear and circular DNA of identical N values displayed different mobilities in a low percentage agarose gel. Relaxed (flexible), circular DNA molecules were prepared by treating a supercoiled DNA ladder mixture with topoisomerase I. A λ DNA–Hind III fragment mixture and a high molecular size DNA marker set provided linear DNA standards in the appropriate chain length range.

When run simultaneously in a 0.6% agarose gel, the circular chains tracked the mobilities of their linear analogs over a broad molecular size range (Fig. 5). However, at molecular sizes above the onset of strong chain entanglement for the linear chains, the data sets diverged. At a lower gel concentration (0.3%), and consequently at lower chain entanglement, data sets for the circular and linear DNA molecules superimposed (Fig. 5). Serwer and Allen (*10*) previously reported that only above a threshold gel concentration did mobilities for relaxed, circular DNA molecules differ from mobilities of linear analogs. Taken together, these observations suggest that mobility in the weakly entangled regime is controlled by N and not by R.

Our results show that both the sieving and reptation theories are inadequate for describing mobilities of weakly entangled, flexible macromolecules. A new theory that correctly predicts equivalent mobilities for star, circular, and linear topologies invokes an entropically regulated transport mechanism. A weakly entangled, flexible polymer chain inside a dilute gel can adopt many different configurations. The chain prefers, in a statistical sense, to remain in environments that allow the greatest degree of configurational freedom; these environments maximize the chain configurational entropy.

In a random gel, such as agarose, there will be regions that are either very dense in gel fibers, or relatively open. The chain will possess the largest number of configurations, and thus the largest entropy, in the open regions. To move between open regions, the polymer chain must squeeze through denser gel regions where the chain entropy is lower; these dense regions act as entropic barriers to translation. The frequency of barrier crossing will control the electrophoretic mobility for intermediate chain length polymers. Very short chains (unentangled) will not be significantly affected by the randomness of the gel since they are always contained in a homogeneous local environment; they will be sieved instead. Longer chains (strongly entangled) will respond to an averaged environment that includes enough dense and open regions so that the chain configuration entropy no longer depends on position in the gel; thus, reptation is a likely mechanism of motion.

Some of the inadequacies of the sieving and reptation models have been discussed (*11, 12*); these studies suggest that spatial variations in the gel environment dictate the rate of electrophoretic migration for weakly entangled chains. Under certain confinement conditions, including those in our experiments, chain configurational entropy becomes an extensive function of N, which is independent of molecular topology (*13*); such independence explains our mobility measurements.

REFERENCES AND NOTES

1. L. S. Lerman and H. L. Frisch, *Biopolymers* **21**, 995 (1982); O. J. Lumpkin and B. H. Zimm, *ibid.*, p. 2315; O. J. Lumpkin, P. Dejardin, B. H. Zimm, *ibid.* **24**, 1573 (1985); G. W. Slater and J. Noolandi, *ibid.* **25**, 431 (1986); J. M. Deutsch, *Science* **240**, 922 (1988); E. O. Shaffer II and M. Olvera de la Cruz, *Macromolecules* **22**, 1351 (1989); J. Melenkevitz and M. Muthukumar, in preparation.
2. G. W. Slater, J. Rosseau, J. Noolandi, C. Turmel, M. Lalande, *Biopolymers* **27**, 509 (1988); G. W. Slater and J. Noolandi, *ibid.* **28**, 1781 (1989).
3. D. Rodbard and A. Chrambach, *Proc. Natl. Acad. Sci. U.S.A.* **65**, 970 (1970); *Anal. Biochem.* **40**, 95 (1971).
4. A. G. Ogston, *Trans. Faraday Soc.* **54**, 1754 (1958).
5. D. L. Smisek and D. A. Hoagland, *Macromolecules* **22**, 2270 (1989).
6. N. C. Stellwagen, *Biopolymers* **24**, 2243 (1985); H. Hervet and C. P. Bean, *ibid.* **26**, 727 (1987).
7. Linear PSS samples were purchased from Pressure Chemical or prepared from polystyrene standards as described (*5*). Three polystyrene star samples (N_{arm} = 540, 1000, and 1400; samples I, II, and III, respectively) were obtained from Polysciences. One additional sample (N_{arm} = 5000; sample IV) was provided by L. Fetters. Samples I, II, and III appear to have been prepared by the so-called "nodule" method as described in G. Quack, L. J. Fetters, N. Hadjichristidis, and R. N. Young [*Ind. Eng. Chem. Prod. Res. Dev.* **19**, 587 (1980)]. This synthesis procedure yields a product mixture containing stars of a single, well-defined arm length; this mixture, however, possesses a broad distribution of f. Sample IV was prepared by a chlorosilane coupling reaction that yields stars of uniform f and N_{arm}. After sulfonation, ^{13}C-NMR measurements show essentially complete substitution at the para position of the phenyl ring. Sulfonation makes the polymers both water-soluble and charged; this process does not modify the star topology of the nodule-based samples. Organosilane linkages may be broken during acid-catalyzed sulfonation, however, so the water-soluble product of sample IV displays a distribution of f (but not of N_{arm}).
8. L. Wang and V. A. Bloomfield, *Macromolecules* **23**, 194 (1990).
9. H. Yamakawa, *Modern Theory of Polymer Solutions* (Harper & Row, New York, 1971) pp. 46–52.
10. P. Serwer and J. L. Allen, *Biochemistry* **23**, 922 (1984).
11. M. Muthukumar and A. Baumgartner, *Macromolecules* **22**, 1937 (1989); *ibid.*, p. 1941.
12. B. H. Zimm, *Phys. Rev. Lett.* **61**, 2965 (1988).
13. A. Halperin and S. Alexander, *Macromolecules* **20**, 1146 (1987).

14. We thank the National Science Foundation Materials Research Laboratory at the University of Massachusetts for financial support, J. Mays for technical assistance with star polymers, and M. Muthukumar and K. McGrath for helpful discussions.

29 November 1989; accepted 22 March 1990